

# Influence of Anodization-Electrolyte Aging on the Photocatalytic Activity of TiO<sub>2</sub> Nanotube Arrays

Luka Suhadolnik,\* Živa Marinko, Maja Ponikvar-Svet, Gašper Tavčar, Janez Kovač, and Miran Čeh



Cite This: *J. Phys. Chem. C* 2020, 124, 4073–4080



Read Online

ACCESS |



Metrics & More

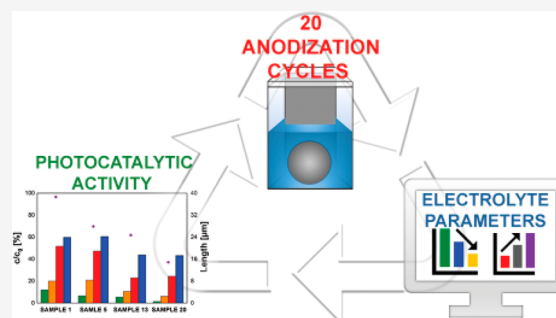


Article Recommendations



Supporting Information

**ABSTRACT:** TiO<sub>2</sub> nanotubular films prepared using the anodic oxidation process applied to various forms of metal titanium are promising materials for photocatalytic applications. However, during successive anodizations in batch-anodization cells, the chemical composition of the NH<sub>4</sub>F- and water-based ethylene glycol electrolyte changes with each subsequent anodization, which greatly affects the final photocatalytic properties of the annealed TiO<sub>2</sub> nanotubular films. In the present study, 20 titanium discs (Φ 90 mm) were sequentially anodized in the same anodization electrolyte. The chemical composition of the electrolyte was measured after each anodization and correlated with the anodization current density, temperature, electrical conductivity, and pH of the electrolyte and with the morphology, structure, composition, and photocatalytic activity of the resulting TiO<sub>2</sub> nanotube films. It was found that the length of the TiO<sub>2</sub> nanotubes decreased with the age of the electrolyte due to its lower conductivity. The subsurface chemical composition was evaluated by time of flight secondary ion mass spectrometry (ToF SIMS) analyses, and the integrated ToF SIMS signals over a depth of 250 nm for the TiO<sub>2</sub> nanotube films showed that the concentration of F<sup>−</sup> in the annealed TiO<sub>2</sub> film increased with each subsequent anodization due to the increased pH value of the electrolyte. As a consequence, the concentration of the OH<sup>−</sup> and O<sub>2</sub><sup>−</sup> species decreased, which is a major reason for the reduced photocatalytic activity of the TiO<sub>2</sub> films. It is proposed that the length of the TiO<sub>2</sub> nanotubes does not play a decisive role in determining the photocatalytic activity of the TiO<sub>2</sub> nanotube films. Finally, the best measured degradation results of 60% for caffeine were thus achieved for the first anodized titanium discs. After that the efficiency gradually decreased for each subsequent anodized disc.



## 1. INTRODUCTION

Anodic oxidation is a well-known process that was first used for the protection of aluminum in the early 20th century. Its main purpose is to increase the adherent strength and the thickness of the film formed by a natural oxidation process.<sup>1</sup> The process is still used in industrial settings for protecting and coloring aluminum.<sup>2</sup> However, with the emergence of nanotechnology, researchers began to modify the anodic oxidation process to produce porous structures that can be used as a template for the synthesis of one-dimensional nanostructures<sup>3,4</sup> or as an immobilized nanostructured film on a metal substrate for various applications.<sup>5,6</sup>

Al<sub>2</sub>O<sub>3</sub> is the most used template material, obtained by the anodization of aluminum,<sup>7</sup> while TiO<sub>2</sub> nanotubes, obtained by the anodization of titanium, are the most investigated materials for the direct use of anodized films. TiO<sub>2</sub> nanotubes have a high surface area and unique electronic, ionic, and biocompatibility properties, which lead to many different applications.<sup>8</sup> Among them, photocatalysis is the most studied and reported in the scientific literature.<sup>9</sup>

The most important characteristics of an efficient TiO<sub>2</sub> photocatalyst are its high activity, low cost, and good stability. Additionally, the ideal photocatalyst should be strongly

adhered to a support enabling a continuous photocatalytic reaction without the need to remove and recycle the photocatalyst.<sup>10</sup> Immobilization can be most easily achieved with the use of an anodic oxidation process, which at the same time allows the low-cost synthesis of TiO<sub>2</sub> nanotube films. Moreover, anodic oxidation enables the optimization of the nanotube morphology by adjusting the anodization conditions.<sup>11</sup>

The influence of the most important anodization parameters (anodization voltage, time of anodization, and electrolyte composition and temperature) on the morphology of TiO<sub>2</sub> nanotubes has been well investigated.<sup>12,13</sup> At the same time, the process of nanotube growth during anodic oxidation is well-known. Water in the electrolyte oxidizes Ti to form TiO<sub>2</sub>. In order to grow nanotubes rather than a compact TiO<sub>2</sub> film, fluoride must be present in the electrolyte. It participates in the TiO<sub>2</sub> etching process and in the complexation of titanium

**Received:** October 10, 2019

**Revised:** January 14, 2020

**Published:** January 21, 2020

cations at the oxide/electrolyte interface.<sup>14</sup> This knowledge enables the synthesis of an immobilized TiO<sub>2</sub> photocatalyst with specific morphological characteristics, which can be used for various applications.<sup>15,16</sup> However, in order for the anodic oxidation of titanium to be used for the industrial production of TiO<sub>2</sub> nanotube films, a comprehensive understanding of the changes in the electrolyte's composition during the anodization process is needed.

Recently, there were a few studies pointing out the lack of reproducibility of the anodization process when titanium metal is repeatedly anodized in a fluoride-containing electrolyte solution. Lee et al. focused on the influence of the electrolyte's conductivity on the formation of TiO<sub>2</sub> nanotube films in a HF-based ethylene glycol electrolyte.<sup>17</sup> The authors tested the resulting anodic films as anodes for dye-sensitized solar cells. Two other research groups have studied the influence of electrolyte aging on the nanotube length and diameter.<sup>18,19</sup> The anodization electrolyte used in both studies was prepared with ethylene glycol, ammonium fluoride, and water. The study by Gulati et al.<sup>19</sup> focused on the anodization of curved titanium surfaces, whereas the study by Sopha et al.<sup>18</sup> determined the influence of electrolyte aging on the anodization of flat titanium foils. In the latter study, an adhesion analysis of the anodized nanotube film was also carried out.

Most of the studies reported in the literature focused primarily on the influence of the electrolyte's aging on the morphological changes to the TiO<sub>2</sub> nanotube films. It has been reported that the anodization electrolyte has to be preanodized in order to prevent the TiO<sub>2</sub> nanotube film's delamination from the substrate, thus improving its mechanical stability.<sup>8</sup> However, the range of electrolyte compositions that allows the synthesis of high-quality immobilized TiO<sub>2</sub> films in a reproducible way has not been yet reported and the electrolyte's aging was not linked to the application-related properties of the grown TiO<sub>2</sub> films.

In the present work, the influence of the anodization electrolyte's aging on its composition was studied. The aging was determined by the number of hours during which the electrolyte was used for anodization. Furthermore, the influence of the changes in the electrolyte's composition on the photocatalytic activity of annealed TiO<sub>2</sub> nanotubes was determined using caffeine as a model degradation molecule. During the anodization, the current–time curves and the electrolyte temperature were recorded. After the anodization, the electrolyte's conductivity was measured and the fluoride and water contents were accurately determined. To the best of our knowledge, the free-fluoride content in an anodization electrolyte that has been used for various times has not been measured and reported before. Additionally, the concentration of negative ions in an annealed TiO<sub>2</sub> film up to a depth of 250 nm was also measured, which is essential for explaining the photocatalytic activity of the anodized films.

## 2. EXPERIMENTAL SECTION

**2.1. Anodic Oxidation of Titanium Discs.** Highly ordered TiO<sub>2</sub> nanotube films were grown in a well-defined anodization setup shown in Figure 1. Titanium foils (200  $\mu$ m thick, 99.8%, Baoji Lyne Metals Co., Ltd.) were first laser cut into discs with a diameter of 98.5 mm. The foils were then cleaned in acetone in an ultrasonic bath, rinsed with ethanol, and dried under a stream of nitrogen. After cleaning, the discs were anodized at a constant potential of 60 V for 6 h in an

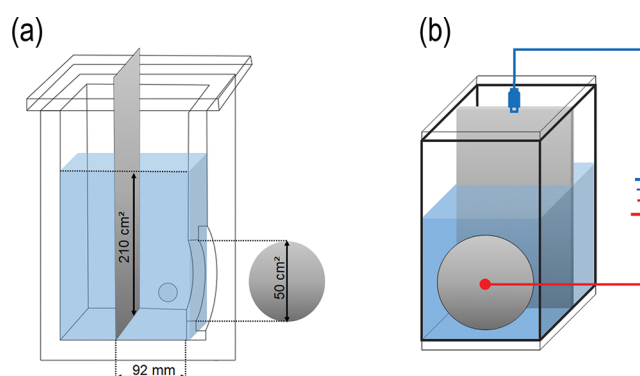


**Figure 1.** Anodization setup in which 20 sequential anodizations were performed. The area of the anodized titanium disc was approximately 50 cm<sup>2</sup>, whereas the area of the stainless-steel cathode immersed into the electrolyte solution was approximately 210 cm<sup>2</sup>. The titanium anode was connected to the positive electric potential while the cathode was connected to the negative one (b). The circle on the back of the anodization cell (a) shows the position of the temperature sensor.

ethylene glycol electrolyte with 0.3 wt % of ammonium fluoride (99.99%, Sigma-Aldrich) and 2 vol % of deionized water. The total volume of the anodization electrolyte at the beginning of the experiments was 2 L. The area of the titanium disc exposed to the electrolyte was fixed at approximately 50 cm<sup>2</sup>; the part of the titanium disc that was exposed to the electrolyte had a diameter of approximately 80 mm. The distance between the titanium anode and the stainless-steel cathode with a surface area of 210 cm<sup>2</sup> was kept constant at 90 mm. There was one anodization a day, and the total number of anodized discs was 20. During each anodization the current–time curve was measured and the electrolyte temperature was monitored throughout the entire procedure. During this time the anodization cell was covered with a lid to minimize the absorption of water from the surrounding air and sealed immediately after the anodization. The as-anodized amorphous titanium discs were washed with deionized water and ethanol and annealed at 450 °C for 1 h in air (heating and cooling at 5 °C min<sup>−1</sup>).

### 2.2. Characterization of the Anodization Electrolyte.

The electrolyte was characterized after each anodization in terms of conductivity and chemical composition. The electrolyte's conductivity was measured with a ProLine Plus M330 conductivity meter immediately after each anodization. The electrolyte's pH was measured before the first and after the last anodization using a benchtop pH meter (Mettler Toledo). The electrolyte samples with a volume of 1 mL were withdrawn before the start of the next anodization when the electrolyte composition reached a steady state (i.e., it was homogeneous throughout the entire volume). The fluoride, ammonia and water contents were determined in corresponding aliquots of the electrolyte sample. A Metrohm model 906 Titrando analyzer and a combined fluoride-ion selective electrode (Thermo Orion, model 9609) were used for the potentiometric determination of the fluoride using the standard addition method with the subtraction of a blank value.<sup>20</sup> The content of water was determined by Karl Fischer titration using a double platinum electrode (ISKRA HEP 0701) and an ISKRA voltmeter (Iskra pH–meter MA 5740).<sup>21</sup> The ammonia content was determined spectrophotometrically using a HACH DR/2010 spectrophotometer.

**2.3. Characterization of the Anodized Films.** The morphological characterization of the anodized titanium discs was carried out in a field-emission scanning electron microscope (FSEM) (Jeol JSM-7600F). The lengths of the nanotubes were estimated from 5 cross-section cuts of the nanotubes of each sample. The structure of  $\text{TiO}_2$  films was characterized with X-ray diffraction (D5000 Bruker AXS diffractometer with  $\text{Cu-K}\alpha$  radiation;  $\lambda = 1.5406 \text{ \AA}$ ) and the surface composition was analyzed with X-ray photoelectron spectroscopy (XPS) on a PHI-TFA XPS spectrometer (Physical Electronics Inc.) equipped with Al-monochromatic source of X-rays. Additionally, surface composition was evaluated by time of flight secondary ion mass spectrometry (ToF SIMS). Mass spectra of positive and negative secondary ions emitted from the surface were acquired by ToF SIMS 5 instrument (ION TOF) using  $\text{Bi}^+$  ion beam of 30 keV for spectra excitation and  $\text{Cs}^+$  ion beam at 2 keV for ion sputtering during depth profile analyses. SIMS spectra were collected during depth profile analyses from the surface to the depth of 250 nm. Integral of specific fragments in SIMS spectra ( $\text{F}^-$ ,  $\text{OH}^-$ ,  $\text{TiO}^-$ ,  $\text{O}_2^-$ ) were calculated and compared.

**2.4. Photocatalytic Degradation of Caffeine.** The photocatalytic efficiency of the  $\text{TiO}_2$  nanotube arrays was investigated by measuring the degradation of caffeine ( $\geq 99.0\%$  HPLC grade, Sigma-Aldrich) with an initial concentration of approximately  $50 \text{ mg L}^{-1}$ . The annealed discs were placed in a Petri dish with 50 mL of the initial caffeine solution and illuminated in a sterilizer (Kambič I-265 CK UV) for 3 h. A sample with a volume of  $200 \mu\text{L}$  was collected after 30 min in the dark and then four times during the illumination time. The experimental setup was evaluated before the photocatalytic degradation tests were made. No concentration gradients were detected despite static experimental conditions being used. The results were also not influenced by the sample-collection location. All the samples were analyzed in a high-precision UV-vis-IR spectrophotometer.

### 3. RESULTS AND DISCUSSION

**3.1. Monitoring the Anodization Process.** The anodic oxidation of the titanium was monitored by measuring the electrical current density, temperature, and electrical conductivity of the electrolyte during the anodization. Additionally, the pH of the electrolyte was measured at the beginning of the anodization experiments and after the last anodization. All these parameters greatly influence the growth of the  $\text{TiO}_2$  nanotubes, their morphology, and properties. Figure 2 shows current density vs time curves during the first 30 min of the anodization of the titanium discs in electrolytes of different ages: 0, 24, 72, and 114 h. The inset in Figure 2 shows the current–time plot for the entire 6 h anodization period together with the average electrolyte temperature during the anodizations. It is evident that the current density drops when the electrolyte is aging after subsequent anodizations. The average current density during the first anodization was more than three times higher than during the 20th ( $136 \text{ mA cm}^{-2}$  compared to  $42 \text{ mA cm}^{-2}$ ). The changes in the current density are the result of changes to the electrolyte's composition. The steady-state current density increases with an increasing fluoride concentration, which strongly influences the morphology of the  $\text{TiO}_2$  nanotubes, since the higher the average current density, the thicker the  $\text{TiO}_2$  film. In a certain range, the film thickness affects its photocatalytic activity. Like the

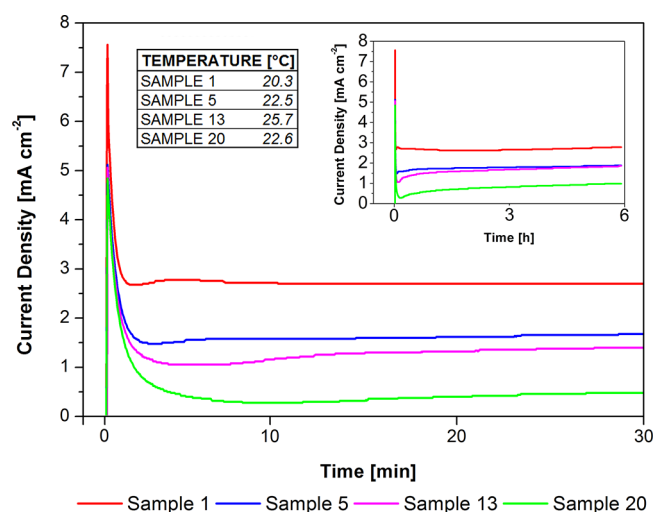


**Figure 2.** Current density vs time measured at the beginning of the anodization of the titanium discs in different aged electrolytes (1st, 5th, 13th, and 20th anodization). (inset) Current density vs time during the entire anodization period, together with average temperature of the anodization electrolyte.

current density, the temperature of the electrolyte during the anodization can strongly influence the morphology of the grown  $\text{TiO}_2$  film.<sup>17</sup> The electrolyte's temperature increases only slightly during anodization, which can increase the current density. However, to what extent does the temperature rise depend on the anodization conditions (especially the applied voltage), the dimensions of the anodization cell (they determine the volume of the electrolyte) and the size (exposed surface area) of the electrodes. In our anodization system there was only slight change in temperature during anodization, and the average electrolyte temperature of the individual anodizations did not differ much (the lowest average temperature was  $20.3 \text{ }^\circ\text{C}$  for the first anodization and the highest  $25.7 \text{ }^\circ\text{C}$  in the 13th anodization), and this did not significantly affect the morphology and photocatalytic properties of the films.

The electrical conductivity of the electrolyte decreased with the increasing number of anodizations (Figure 3), which is due to the consumption of  $\text{F}^-$  ions and  $\text{NH}_4^+$  ions during the

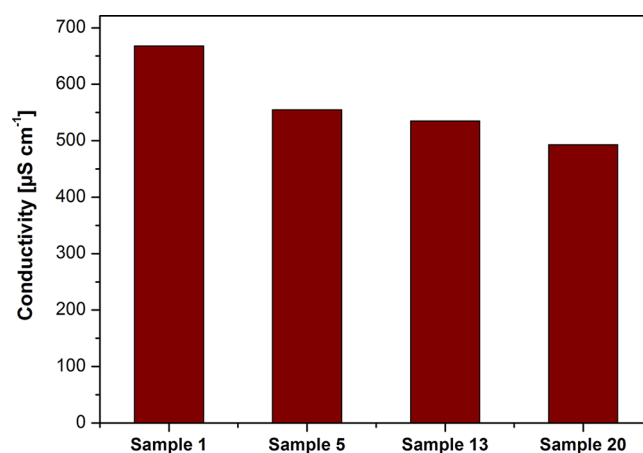


**Figure 3.** Conductivity of anodization electrolyte measured immediately after the anodic oxidation of samples 5, 13, and 20 and of the starting electrolyte (sample 0).



anodization process. Fluoride ions have two main effects on the oxide-formation process. First, they form water-soluble  $[\text{TiF}_6]^{2-}$  ions and prevent the formation of hydroxide. Second, they etch the formed  $\text{TiO}_2$  so that a nanotubular layer is formed instead of a compact one.<sup>14</sup> Since the fluoride ions induce the chemical dissolution reaction and possess a small ionic radius, a small fraction of fluoride ions can be incorporated into the amorphous  $\text{TiO}_2$ .<sup>22,23</sup>

The as-grown  $\text{TiO}_2$  nanotubes are mostly amorphous and have to be transformed to the anatase crystalline phase in order to be photocatalytically active. During annealing in air above 280 °C, most of the fluoride is removed in the form of HF from the  $\text{TiO}_2$  film.<sup>22</sup> The remaining fluoride was measured with the ToF SIMS analysis of the annealed film; however, it was determined that it is almost completely removed in the case of annealing at 700 °C.<sup>24</sup> The concentration of ammonium ions also influences the morphology of the  $\text{TiO}_2$  nanotubes.<sup>25</sup> They are consumed during the anodization process due to the formation of the  $(\text{NH}_4)_2\text{TiF}_6$  salt,<sup>26</sup> followed by the formation of ammonia ( $\text{NH}_3$ ), which is volatile under alkaline conditions (eq 2). The pH of the unused electrolyte was  $5.5 \pm 0.3$ , whereas the pH of the electrolyte used for 20 anodizations was  $8.5 \pm 0.4$ , due to the formation of ammonia and the electrolysis of the water on the cathode, according to the following equation

Reaction between the  $\text{NH}_4\text{F}$  and  $\text{TiO}_2$  and the formation of the  $(\text{NH}_4)_2\text{TiF}_6$  salt



It has been reported that the pH of the electrolyte influences the structure, morphology, and photoresponse of the  $\text{TiO}_2$  nanotube arrays.<sup>27,28</sup> The current density during anodization is higher when it is performed in an acidic electrolyte. This results in a thicker and denser oxide film.<sup>29</sup> The change in the electrical conductivity is most noticeable after the first anodization, since it decreases from  $668 \text{ mS cm}^{-1}$  (measured before the first anodization) to  $561 \text{ mS cm}^{-1}$  (measured after the second anodization), then it decreases very slowly. It was observed that the concentrations of  $\text{NH}_4^+$  and  $\text{F}^-$  ions are not the only ones that influence the electrolyte's conductivity. The compounds that are formed during the anodization process also play an important role, since the Ti and F ions form salts. The electrolyte's conductivity influences the current density during the anodization and thus the growth rate of the  $\text{TiO}_2$  nanotubes and their properties. Our results for the electrolyte's conductivity are in accordance with some authors;<sup>19,30</sup> however, not all the authors found that with an increasing number of anodizations the electrolyte's conductivity decreases.<sup>17,18</sup>

**3.2. Analysis of the Anodization Electrolyte's Composition.** The starting electrolyte that was used in the experiments consisted of ethylene glycol with 0.3 wt % ammonium fluoride and 2 vol % deionized water. The measurements of the electrolyte's composition after the anodizations showed that  $\text{F}^-$  ions and  $\text{NH}_4^+$  ions were consumed during each anodization (Figure 4, Table 1). The water content increased over time, since ethylene glycol is relatively hygroscopic and tends to take up water from the surrounding air.<sup>10</sup> The concentration of water increased by about 35%, despite the fact that the anodization cell was covered during every anodization and sealed in between the individual anodizations. The increase in water content in the

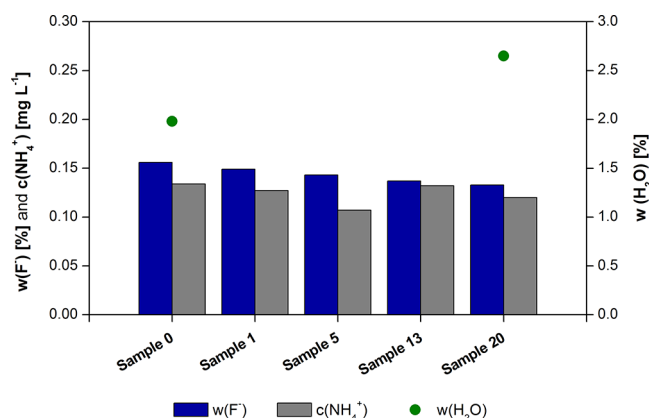


**Figure 4.** Water content and concentration of ammonium and fluoride ions in the anodization electrolyte used for the anodization of an increasing number of samples. Sample 0 represents the starting electrolyte.

**Table 1. Concentration of Ammonium and Fluoride Ions, Together with the Water Content, in the Anodization Electrolyte Used for an Increasing Number of Samples**

sample	0	1	5	13	20
w(F) <sup>−</sup> [%]	0.156	0.149	0.143	0.137	0.133
c(NH <sub>4</sub> <sup>+</sup> ) [mg L <sup>−1</sup> ]	0.134	0.127	0.107	0.132	0.120
w(H <sub>2</sub> O) [%]	1.98	no data	no data	no data	2.65

electrolyte causes the formation of an initial thick compact oxide layer that also reduces the growth rate of the  $\text{TiO}_2$  nanotubes.<sup>31</sup>

As shown in Table 1, the concentration of  $\text{F}^-$  decreases with the increasing number of anodizations. A similar trend is observed for the concentration of  $\text{NH}_4^+$ , except that the measured values fluctuate considerably. Nevertheless, it can be concluded that  $\text{NH}_4^+$  is also consumed during the anodization process, most probably as the volatile, gaseous ammonia evaporates from the anodizing electrolyte. Lim et. al found that uniform nanotubes can be formed at a  $\text{NH}_4\text{F}$  content of 0.25–1.0 wt %.<sup>32</sup> However, our results show that changes in  $\text{NH}_4\text{F}$  concentration result in noticeable morphological changes to the  $\text{TiO}_2$  film, although the  $\text{NH}_4\text{F}$  concentration did not fall below 0.25 wt %. The reason for this is the changes in the electrolyte's pH. At higher pH, the formation of the  $(\text{NH}_4)_2\text{TiF}_6$  salt is reduced, and the nanotubes' morphologies (surface structure, pore diameter, wall thickness, length) are altered.<sup>29</sup> The most noticeable changes in the film's general appearance began with the 17th anodization, as two different morphologies were easily distinguished, even at very low magnifications (Figure S1). The reason for this could be the presence of dissolved titanium salts that disrupt the anodization process when their concentration is too high.

**3.3. Structure, Composition, and Morphology of the  $\text{TiO}_2$  Nanotube Films.** The XRD analysis of the annealed nanotubes films showed that the films are polycrystalline in nature and that all the peaks corresponding to the  $\text{TiO}_2$  anatase crystal structure are clearly resolved (Figure S2). The additional XRD peaks in all the spectra correspond to the metal titanium substrate. The visibility of the Ti peaks depends on the thickness of the  $\text{TiO}_2$  film. The comparison of the highest intensity peaks for the  $\text{TiO}_2$  and Ti ratios and also the absolute  $\text{TiO}_2$  peak intensities (all the XRD spectra were recorded under same conditions) confirm that the  $\text{TiO}_2$  film

(sample 1) is the thickest and that each subsequent anatase TiO<sub>2</sub> film is thinner.

The XPS spectra acquired from the surface of the TiO<sub>2</sub> films (samples 1 and 20) did not show any major differences. Signals of Ti 2p, O 1s, and C 1s are present in all spectra and composition of the surfaces between these TiO<sub>2</sub> films does not differ significantly (Figure S3). The XPS valence band spectra are also similar (Figure S4). The estimated valence band maxima are approximately 2.9 eV for all samples. However, the ToF SIMS analysis which is much more sensitive than XPS analysis (analyzing the region from the surface to depth of 250 nm) of the F<sup>−</sup> content showed that sample 1 contained much less F<sup>−</sup> than sample 20 (Figure S5). This could be due to the acidic pH of  $5.5 \pm 0.3$  during the first anodization and the basic pH of  $8.5 \pm 0.4$  during the last anodizations. This is because the acidic pH mainly causes the formation of TiF<sub>6</sub><sup>2−</sup> ions, while different oxofluorides are formed at the basic pH. The TiF<sub>6</sub><sup>2−</sup> ions are soluble in the anodization electrolyte in comparison with the less soluble oxofluorides, which to a greater extent remain in the TiO<sub>2</sub> film.

Figures 5 and 6 show the top surfaces of the anodized titanium discs annealed at 450 °C. SEM micrographs of one

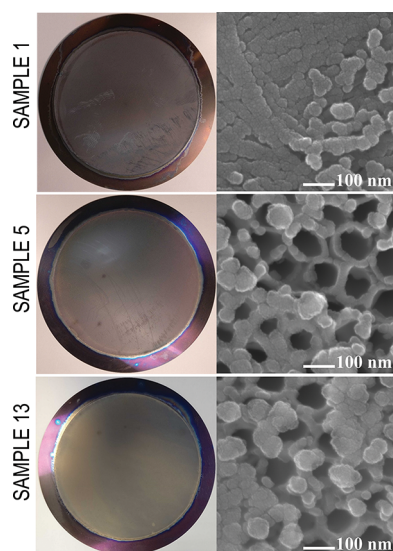


**Figure 5.** Top surface of anodized titanium discs (samples 1, 5, 13): photographs (left column) and high-magnification SEM images (right column).

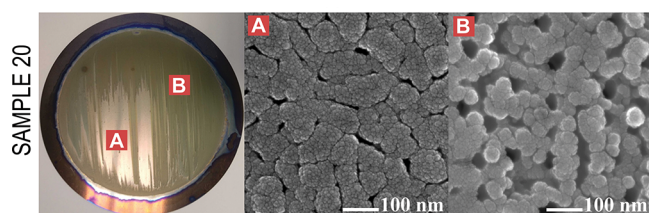


**Figure 6.** Top surface of anodized sample 20: photograph (left-hand side) and high-magnification SEM images (right-hand side). Two distinctive areas are observed: one with the formed TiO<sub>2</sub> nanotubes (B) and areas where only a compact TiO<sub>2</sub> film is present (A).

unannealed sample are shown in Figure S6. Since unannealed samples are amorphous, the surface does not show any distinct features as compared to annealed samples. The photographs of the discs in Figures 5 and 6 show the macroscopic appearance

of the films, while the SEM images reveal the morphological characteristics of their surfaces. Four samples are shown. The results indicate that the top surfaces of the TiO<sub>2</sub> films vary greatly. The anodization of the first sample resulted in nanotubes with an almost completely closed top surface, due to the excessive etching and the “nanograss” formation on the top surface of the sample (Figure S7). The top surface of the first sample does not show any visible irregularities. These only appeared during and after the 17th anodization, when there were regions that appeared polished and free of any oxide film. These regions became more pronounced with each subsequent anodization and are shown for sample 20. In Figure 6, regions A and B are clearly distinguished even at low magnifications. The SEM micrographs of these regions reveal that the entire sample is anodized, but the morphology in region A differs from that in B. The morphology of the top surface of the TiO<sub>2</sub> film in region B is very similar to that of sample 1. The top surface of the nanotube film is almost completely closed. The morphology of the film in region A is not typical for anodized titanium, as a compact spongelike oxide was formed instead of the nanotubes. The top surfaces of samples 5 and 13 consist of very open nanotubes with a diameter of approximately 100 nm. We found that the anodization electrolyte’s pH has an important influence on the morphology of the nanotube film, and it slowly increased during the experiments. It is known from the literature that morphologically the most uniform and consistent nanotubes are grown in a neutral electrolyte medium,<sup>28</sup> which is consistent with our results. A slightly acidic or alkaline electrolyte caused a structural disorder of the top surface of the nanotubes, which were relatively closed. When the pH of the electrolyte was in the neutral region, the top surface of the nanotubes was more regular and open. This occurred in the case of the fifth anodization.

**3.4. Caffeine Degradation.** The photocatalytic activity of the TiO<sub>2</sub> nanotube arrays was determined by measuring the degradation of caffeine. Figure 7 shows the degradation of caffeine using four different samples after different reaction times. The same figure also shows the length of the TiO<sub>2</sub> nanotubes for all four samples. The length of nanotubes was measured from cross-sectional SEM images (Figure S8).

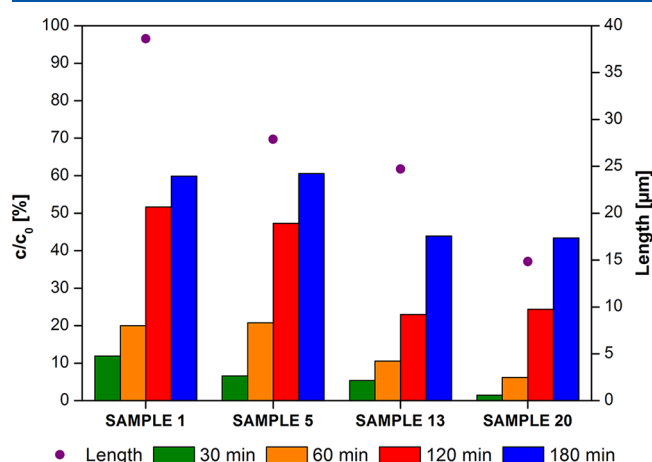


**Figure 7.** Photocatalytic degradation of caffeine using anodized titanium discs (samples 1, 5, 13, and 20). The average TiO<sub>2</sub> nanotube film thickness (dots and the legend on the right-hand y-axis) is also shown for these samples.

Samples 1 and 5 show similar activity, i.e., a degradation of approximately 60% of the initial caffeine during a UV illumination period of 3 h. Samples 13 and 20 have a poorer photocatalytic performance. Both samples achieved a degradation of approximately 44% of the caffeine after the longest reaction time. In order to better describe the achieved caffeine conversions, the photonic efficiencies ( $\xi$ ) and initial reaction rates ( $R_i$ ) were calculated using the equations described by Krivec et al.<sup>10</sup> Photonic efficiency is defined as the number of transformed reactant molecules divided by the number of incident photons of monochromatic light. It was calculated with eq 2, while the initial reaction rate was calculated from eq 3.

$$\xi = \frac{\Delta c V}{I_0 \Delta t A}, \quad \text{where } I_0 = \frac{I \lambda}{N_a h c} \quad (2)$$

$$R_i = \frac{\Delta c}{N_a \Delta t} \quad (3)$$

$\Delta c$  is the difference in caffeine concentration in reaction time  $\Delta t$ .  $V$  is the volume of the caffeine solution,  $A$  is the geometric surface area, and  $I_0$  is photon flux. It is calculated from UV light intensity  $I$  (1.097 mW cm<sup>-1</sup> during our experiments), wavelength of UV light  $\lambda$ , Avogadro's constant  $N_a$ , Planck constant  $h$ , and the speed of light  $c$ . The best photonic efficiency was approximately 0.43%, achieved with sample 5. The largest number of incident photons was lost during the photocatalytic reaction on the surface of sample 20, whose photonic efficiency was approximately 0.31%. The initial reaction rates followed the same order. The best achieved  $R_i$  was approximately  $0.014 \times 10^{-6}$  mol L<sup>-1</sup> s<sup>-1</sup>. The photonic efficiencies and the initial reaction rates of samples 1, 5, 13, and 20 are shown in the Supporting Information (Figure S9). It is known from the literature that the photocatalytic activity is influenced by the morphology and the length of the TiO<sub>2</sub> nanotubes, whereby the photodegradation efficiency is improved with increasing lengths of the nanotubes, due to higher surface area and the increased light absorption.<sup>33</sup> However, the photocatalytic activity is enhanced only to a certain extent, since there exists a limited penetration depth of UV light.<sup>34</sup> The longer nanotubes have thinner walls and greater volumes in the upper part of the tubes, meaning that the UV light has to travel on a longer pathway before absorption and the production of electron–hole pairs.<sup>35</sup> According to the data in the literature, many authors observed that the best photocatalytic results were obtained with TiO<sub>2</sub> nanotubes of different lengths. The following optimum nanotube lengths were reported: 2.2,<sup>34</sup> 4.8,<sup>33</sup> and 7  $\mu$ m.<sup>35</sup> Irrespective of all the literature data, our results show that the length of the nanotubes, when comparing samples that were anodized with different ages of electrolytes, is not the decisive parameter in determining the photocatalytic activity of the TiO<sub>2</sub> films. The reason why the thickness of the TiO<sub>2</sub> film does not significantly influence its photocatalytic activity is that our thinnest film (measured for sample 20) already has had a thickness of approximately 15  $\mu$ m, which is more than the most often reported optimum thickness for the nanotube films. The longest TiO<sub>2</sub> nanotubes were grown during the first anodization, when the electrolyte was still fresh and its conductivity was the highest. The length of the nanotubes after 6 h of anodization was approximately 40  $\mu$ m. Our findings regarding the effect of the nanotubes' morphology and length

on their photocatalytic activity are in accordance with a study conducted by Mabiala Masiala et al. using H<sub>2</sub>SO<sub>4</sub>- and NaOH-based anodization electrolytes. Those authors reported that anodization in acid electrolytes results in stable oxide films with improved adhesion to the titanium metal substrate and an improved photoresponse.<sup>27</sup> Our results show a gradual decrease in the photocatalytic efficiency with the aging of the electrolyte due to an increase of the electrolyte's pH. Furthermore, the differences in the intensities of the OH<sup>-</sup>, O<sub>2</sub><sup>-</sup>, and TiO<sup>-</sup> signals observed from the ToF SIMS analyses of samples 1 and 20 (Figure 8) also explain the differences in

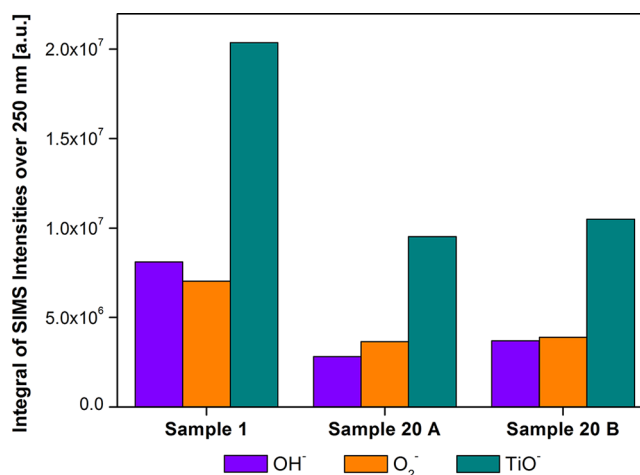


**Figure 8.** Integrals of SIMS signals of OH<sup>-</sup>, O<sub>2</sub><sup>-</sup>, and TiO<sup>-</sup> ions over a depth of 250 nm for samples 1 and 20. Regions A and B of sample 20 were analyzed.

the photocatalytic activities of all the samples. The signal intensities of all three negative ionic fragments follow the same trend as the photocatalytic efficiencies of the samples. The intensities observed for sample 1 are higher than for sample 20. The obtained results are in accordance with the literature data. Since the photocatalytic oxidation of caffeine proceeds via hydroxyl radicals,<sup>36</sup> the concentration of the surface OH<sup>-</sup> greatly influences the activity of the catalyst. In sample 20, the concentration of the surface OH<sup>-</sup> is reduced due to the fluoride-exchange. It can be seen in Figure S3 that the amount of F<sup>-</sup> in the nanotube films increases after the first anodization. The difference in the intensity of the TiO<sup>-</sup> and O<sub>2</sub><sup>-</sup> species does not play a role in the photocatalytic reactions. Due to the bombardment of the primary ion beam of bismuth during the ToF SIMS analysis, there is a desorption of TiO<sup>-</sup> and O<sub>2</sub><sup>-</sup> species originating from the TiO<sub>2</sub> structure. However, some of the oxygen (O<sub>2</sub><sup>-</sup>) could also represent the oxygen adsorbed as superoxo which plays an important role in the catalytic oxidation reactions.<sup>37</sup>

Figure 9 summarizes the results and correlates the changes in the electrolyte composition due to repeated anodizations with the growth of the TiO<sub>2</sub> nanotubes and their photocatalytic activity. It can be concluded that changes in the electrolyte's composition negatively affect the growth rate of the nanotubes and their photocatalytic properties. The electrolyte's pH is gradually increasing, which plays a very important role.



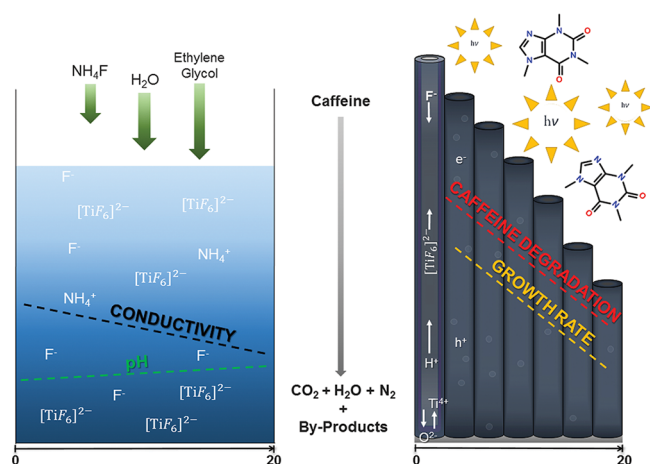


**Figure 9.** Effect of repeated anodic oxidations in the same electrolyte on the anodization electrolyte's composition and conductivity, as well as on the growth rate and photocatalytic activity of the grown  $\text{TiO}_2$  nanotubes.

## 5. CONCLUSIONS

We studied the influence of an anodization electrolyte's aging after sequential anodizations with respect to the morphology, structure, composition, and photocatalytic activity of  $\text{TiO}_2$  nanotube films. Twenty titanium foils were anodized in the same electrolyte to grow rigidly attached  $\text{TiO}_2$  nanotube films. The samples were then annealed to transform the amorphous  $\text{TiO}_2$  to the anatase structure. As a general rule, it was found that with each subsequent anodization the length of the  $\text{TiO}_2$  nanotubes gradually decreased, as did the corresponding photocatalytic activities of the formed  $\text{TiO}_2$  films. A microstructural characterization further revealed that the last anodized discs, apart from the areas of formed  $\text{TiO}_2$  nanotubes, also contained areas where only a compact  $\text{TiO}_2$  film was present. The electrolyte's aging was monitored by analyzing its chemical composition after each anodization and by measuring the current density and the temperature during the anodization, as well as the conductivity and pH of the electrolyte. It was determined that the conductivity of the electrolyte was decreasing with each anodization, while the pH value was increasing. Although the concentration of  $\text{F}^-$  in the electrolyte after each subsequent anodization did not change significantly, an integrated ToF SIMS signal over a depth of 250 nm showed that the  $\text{F}^-$  ions did incorporate into the  $\text{TiO}_2$  films and that the concentration of  $\text{F}^-$  in the last anodized disc was approximately three times higher than for the first disc (Figure S3). On the other hand, the concentration of  $\text{OH}^-$  and  $\text{O}_2^-$  in the annealed  $\text{TiO}_2$  films showed the opposite trend. It was concluded that a reduced concentration of  $\text{OH}^-$  and  $\text{O}_2^-$  species at the  $\text{TiO}_2$  surface was the main factor responsible for the reduced photocatalytic activity of the  $\text{TiO}_2$  films after successive anodizations and that the decreased length of the  $\text{TiO}_2$  nanotubes after each anodization does not have a significant effect on the photocatalytic activity of the  $\text{TiO}_2$  films. Moreover, the length of the  $\text{TiO}_2$  nanotubes is primarily governed by the current density, which is a consequence of the electrolyte's conductivity. Our results also suggest that batch-type anodization cells cannot yield reproducible  $\text{TiO}_2$  nanotube films due to aging of the anodization electrolyte and that a continuous regeneration of the anodization electrolyte is needed to obtain  $\text{TiO}_2$  films with comparable photocatalytic activities.

## ■ ASSOCIATED CONTENT

### Supporting Information

The Supporting Information is available free of charge at <https://pubs.acs.org/doi/10.1021/acs.jpcc.9b09522>.

Additional figures showing photograph of annealed anodized film, XRD and XPS spectra of anodized films, amount of  $\text{F}^-$  in annealed nanotubes and anodization electrolyte, SEM image of unannealed sample, top surface of sample 1, and cross-section of the  $\text{TiO}_2$  films (PDF)

## ■ AUTHOR INFORMATION

### Corresponding Author

**Luka Suhadolnik** – Department for Nanostructured Materials, Jožef Stefan Institute, SI-1000 Ljubljana, Slovenia; [orcid.org/0000-0002-9103-6687](https://orcid.org/0000-0002-9103-6687); Phone: +386 1 477 3931; Email: [luka.suhadolnik@ijs.si](mailto:luka.suhadolnik@ijs.si)

### Authors

**Ziva Marinko** – Department for Nanostructured Materials, Jožef Stefan Institute, SI-1000 Ljubljana, Slovenia; Jožef Stefan International Postgraduate School, SI-1000 Ljubljana, Slovenia  
**Maja Ponikvar-Svet** – Department of Inorganic Chemistry and Technology, Jožef Stefan Institute, SI-1000 Ljubljana, Slovenia  
**Gasper Tavcar** – Department of Inorganic Chemistry and Technology, Jožef Stefan Institute, SI-1000 Ljubljana, Slovenia; [orcid.org/0000-0001-9891-6153](https://orcid.org/0000-0001-9891-6153)  
**Janez Kovac** – Department of Surface Engineering and Optoelectronics, Jožef Stefan Institute, SI-1000 Ljubljana, Slovenia  
**Miran Čeh** – Department for Nanostructured Materials, Jožef Stefan Institute, SI-1000 Ljubljana, Slovenia

Complete contact information is available at:

<https://pubs.acs.org/doi/10.1021/acs.jpcc.9b09522>

### Notes

The authors declare no competing financial interest.

## ■ ACKNOWLEDGMENTS

The provision of financial support for the research and the preparation of the manuscript by the Slovenian Research Agency (ARRS) within the research programs P2-0084, P1-0045, and P2-0082 is gratefully acknowledged. This project has also received funding from the European Union's Horizon 2020 research and innovation programme under grant agreement No 823717-ESTEEM3.

## ■ REFERENCES

- (1) Donaldson Craig, J. Anodic Oxidation of Aluminium and Its Alloys. *J. R. Aeronaut. Soc.* **1938**, 42 (331), 603–612.
- (2) Donahue, C. J.; Exline, J. A. Anodizing and Coloring Aluminum Alloys. *J. Chem. Educ.* **2014**, 91 (5), 711–715.
- (3) O'Sullivan, J. P.; Wood, G. C. The Morphology and Mechanism of Formation of Porous Anodic Films on Aluminium. *Proc. R. Soc. London, Ser. A* **1970**, 317 (1531), 511.
- (4) Furneaux, R. C.; Rigby, W. R.; Davidson, A. P. The Formation of Controlled-Porosity Membranes from Anodically Oxidized Aluminium. *Nature* **1989**, 337, 147.
- (5) Macak, J. M.; Tsuchiya, H.; Schmuki, P. High-Aspect-Ratio  $\text{TiO}_2$  Nanotubes by Anodization of Titanium. *Angew. Chem., Int. Ed.* **2005**, 44 (14), 2100–2102.
- (6) Kim, S. J.; Choi, J. Self-Assembled Arrays of ZnO Stripes by Anodization. *Electrochem. Commun.* **2008**, 10 (1), 175–179.

- (7) Chen, Y.-Y.; Yu, B.-Y.; Wang, J.-H.; Cochran, R. E.; Shyue, J.-J. Template-Based Fabrication of SrTiO<sub>3</sub> and BaTiO<sub>3</sub> Nanotubes. *Inorg. Chem.* **2009**, *48* (2), 681–686.
- (8) Roy, P.; Berger, S.; Schmuki, P. TiO<sub>2</sub> Nanotubes: Synthesis and Applications. *Angew. Chem., Int. Ed.* **2011**, *50* (13), 2904–2939.
- (9) Zhou, X.; Liu, N.; Schmuki, P. Photocatalysis with TiO<sub>2</sub> Nanotubes: “Colorful” Reactivity and Designing Site-Specific Photocatalytic Centers into TiO<sub>2</sub> Nanotubes. *ACS Catal.* **2017**, *7* (5), 3210–3235.
- (10) Krivec, M.; Žagar, K.; Suhadolnik, L.; Čeh, M.; Dražić, G. Highly Efficient TiO<sub>2</sub>-Based Microreactor for Photocatalytic Applications. *ACS Appl. Mater. Interfaces* **2013**, *5* (18), 9088.
- (11) Haring, A.; Morris, A.; Hu, M. Controlling Morphological Parameters of Anodized Titania Nanotubes for Optimized Solar Energy Applications. *Materials* **2012**, *5* (10), 1890–1909.
- (12) Nischk, M.; Mazierski, P.; Gazda, M.; Zaleska, A. Ordered TiO<sub>2</sub> Nanotubes: The Effect of Preparation Parameters on the Photocatalytic Activity in Air Purification Process. *Appl. Catal., B* **2014**, *144*, 674–685.
- (13) Qin, L.; Chen, Q.; Lan, R.; Jiang, R.; Quan, X.; Xu, B.; Zhang, F.; Jia, Y. Effect of Anodization Parameters on Morphology and Photocatalysis Properties of TiO<sub>2</sub> Nanotube Arrays. *J. Mater. Sci. Technol.* **2015**, *31* (10), 1059–1064.
- (14) Macak, J. M.; Tsuchiya, H.; Ghicov, A.; Yasuda, K.; Hahn, R.; Bauer, S.; Schmuki, P. TiO<sub>2</sub> Nanotubes: Self-Organized Electrochemical Formation, Properties and Applications. *Curr. Opin. Solid State Mater. Sci.* **2007**, *11* (1), 3–18.
- (15) Sreekantan, S.; Saharudin, K. A.; Wei, L. C. Formation of TiO<sub>2</sub> Nanotubes via Anodization and Potential Applications for Photocatalysts, Biomedical Materials, and Photoelectrochemical Cell. *IOP Conf. Ser.: Mater. Sci. Eng.* **2011**, *21* (1), 012002.
- (16) Lv, H.; Li, N.; Zhang, H.; Tian, Y.; Zhang, H.; Zhang, X.; Qu, H.; Liu, C.; Jia, C.; Zhao, J.; et al. Transferable TiO<sub>2</sub> Nanotubes Membranes Formed via Anodization and Their Application in Transparent Electrochromism. *Sol. Energy Mater. Sol. Cells* **2016**, *150*, 57–64.
- (17) Lee, K.; Kim, J.; Kim, H.; Lee, Y.; Tak, Y.; Kim, D.; Schmuki, P. Effect of Electrolyte Conductivity on the Formation of a Nanotubular TiO<sub>2</sub> Photoanode for a Dye-Sensitized Solar Cell. *J. Korean Phys. Soc.* **2009**, *54* (3), 1027–1031.
- (18) Sopha, H.; Hromadko, L.; Nechvilova, K.; Macak, J. M. Effect of Electrolyte Age and Potential Changes on the Morphology of TiO<sub>2</sub> Nanotubes. *J. Electroanal. Chem.* **2015**, *759*, 122–128.
- (19) Gulati, K.; Santos, A.; Findlay, D.; Losic, D. Optimizing Anodization Conditions for the Growth of Titania Nanotubes on Curved Surfaces. *J. Phys. Chem. C* **2015**, *119* (28), 16033–16045.
- (20) Ponikvar, M.; Stibilj, V.; Žemva, B. Daily Dietary Intake of Fluoride by Slovenian Military Based on Analysis of Total Fluorine in Total Diet Samples Using Fluoride Ion Selective Electrode. *Food Chem.* **2007**, *103* (2), 369–374.
- (21) Vogel, A. I.; Bassett, J. *Vogel's Textbook of Quantitative Inorganic Analysis: Including Elementary Instrumental Analysis*; Longman, 1978.
- (22) Indira, K.; Mudali, U. K.; Nishimura, T.; Rajendran, N. A Review on TiO<sub>2</sub> Nanotubes: Influence of Anodization Parameters, Formation Mechanism, Properties, Corrosion Behavior, and Biomedical Applications. *J. Bio-Tribo-Corrosion* **2015**, *1* (4), 28.
- (23) Peng, Z.; Ni, J. Surface Properties and Bioactivity of TiO<sub>2</sub> Nanotube Array Prepared by Two-Step Anodic Oxidation for Biomedical Applications. *R. Soc. Open Sci.* **2019**, *6* (4), 181948.
- (24) Chung, E. H.; Baek, S. R.; Yu, S. M.; Kim, J. P.; Hong, T. E.; Kim, H. G.; Bae, J.-S.; Jeong, E. D.; Khan, F. N.; Jung, O. Self-Organized TiO<sub>2</sub> Nanotube Arrays in the Photocatalytic Degradation of Methylene Blue under UV Light Irradiation. *J. Korean Phys. Soc.* **2015**, *66* (7), 1135–1139.
- (25) Shankar, K.; Mor, G. K.; Fitzgerald, A.; Grimes, C. A. Cation Effect on the Electrochemical Formation of Very High Aspect Ratio TiO<sub>2</sub> Nanotube Arrays in Formamide–Water Mixtures. *J. Phys. Chem. C* **2007**, *111*, 21.
- (26) Raja, K. S.; Gandhi, T.; Misra, M. Effect of Water Content of Ethylene Glycol as Electrolyte for Synthesis of Ordered Titania Nanotubes. *Electrochem. Commun.* **2007**, *9* (5), 1069–1076.
- (27) Mabilia Masiala, T.; Bantu, A. K. M.; Bakambo, G. E.; Lunguya, J. M.; Kanza, J. L. K.; Muamba, O. M. Influence of PH Preparation on the Photo-Response of Electrodeposited Titanium Dioxide TiO<sub>2</sub> Thin Films. *Int. J. Mater. Sci. Appl.* **2016**, *5* (5), 207.
- (28) Joseph, S.; David, T. M.; Ramesh, C.; Sagayaraj, P. The Role of Electrolyte PH in Enhancing the Surface Morphology of TiO<sub>2</sub> Nanotube Arrays Grown on Ti Substrate. *Int. J. Sci. Eng. Res.* **2014**, *5*, 85–91.
- (29) Sreekantan, S.; Lockman, Z.; Hazan, R.; Tasbihi, M.; Tong, L. K.; Mohamed, A. R. Influence of Electrolyte PH on TiO<sub>2</sub> Nanotube Formation by Ti Anodization. *J. Alloys Compd.* **2009**, *485* (1–2), 478–483.
- (30) Jarosz, M.; Pawlik, A.; Kapusta-Kołodziej, J.; Jaskuła, M.; Sulka, G. D. Effect of the Previous Usage of Electrolyte on Growth of Anodic Titanium Dioxide (ATO) in a Glycerol-Based Electrolyte. *Electrochim. Acta* **2014**, *136*, 412–421.
- (31) Li, H.; Ding, M.; Jin, J.; Sun, D.; Zhang, S.; Jia, C.; Sun, L. Effect of Electrolyte Pretreatment on the Formation of TiO<sub>2</sub> Nanotubes: An Ignored yet Non-Negligible Factor. *ChemElectroChem* **2018**, *5* (7), 1006–1012.
- (32) Ying Chin, L.; Zainal, Z.; Khusaimi, Z.; Sarah Ismail, S. *Electrochemical Synthesis of Ordered Titania Nanotubes in Mixture of Ethylene Glycol and Glycerol Electrolyte*; 2016; Vol. 20.
- (33) Adán, C.; Marugán, J.; Sánchez, E.; Pablos, C.; van Grieken, R. Understanding the Effect of Morphology on the Photocatalytic Activity of TiO<sub>2</sub> Nanotube Array Electrodes. *Electrochim. Acta* **2016**, *191*, 521–529.
- (34) Wang, W.-Y.; Chen, B.-R. Characterization and Photocatalytic Activity of TiO<sub>2</sub> Nanotube Films Prepared by Anodization. *Int. J. Photoenergy* **2013**, *2013*, 1–12.
- (35) Marien, C. B. D.; Cottineau, T.; Robert, D.; Drogui, P. TiO<sub>2</sub> Nanotube Arrays: Influence of Tube Length on the Photocatalytic Degradation of Paraquat. *Appl. Catal., B* **2016**, *194*, 1–6.
- (36) Dalmazio, I.; Santos, L. S.; Lopes, R. P.; Eberlin, M. N.; Augusta, R. *Environ. Sci. Technol.* **2005**, *39*, 5982.
- (37) Setvín, M.; Aschauer, U.; Scheiber, P.; Li, Y.-F.; Hou, W.; Schmid, M.; Selloni, A.; Diebold, U. Reaction of O<sub>2</sub> with Subsurface Oxygen Vacancies on TiO<sub>2</sub> Anatase. *Science* **2013**, *341* (6149), 988–991.